

Mice That Produce ApoB100 Lipoproteins in the RPE Do Not Develop Drusen yet Are Still a Valuable Experimental System

Masashi Fujihara, Marisol Cano, and James T. Handa

Wilmer Eye Institute, Johns Hopkins School of Medicine, Baltimore, Maryland, United States

Correspondence: James T. Handa, 400 N. Broadway, Smith Building, Room 3015, Johns Hopkins University School of Medicine, Baltimore, MD 21287, USA; jthanda@jhmi.edu.

Submitted: July 9, 2014
Accepted: October 3, 2014

Citation: Fujihara M, Cano M, Handa JT. Mice that produce ApoB100 lipoproteins in the RPE do not develop drusen yet are still a valuable experimental system. *Invest Ophthalmol Vis Sci.* 2014;55:7285-7295. DOI: 10.1167/iovs.14-15195

PURPOSE. Mice typically produce apolipoprotein B (apoB)-48 and not apoB100. Apolipoprotein B100 accumulates in Bruch's membrane prior to basal deposit and drusen formation during the onset of AMD, raising the possibility that they are a trigger for these Bruch's membrane alterations. The purpose herein, was to determine whether mice that predominantly produce apoB100 develop features of AMD.

METHODS. The eyes of mice that produce apoB100 were examined for apoB100 synthesis, cholesteryl esterase/filipin labeling for cholesteryl esters, and transmission electron microscopy for lipid particles and phenotype.

RESULTS. Apolipoprotein B100 was abundant in the RPE-choroid of apoB100, but not wild-type mice by Western blot analysis. The apolipoprotein B100,³⁵S-radiolabeled and immunoprecipitated from RPE explants, confirmed that apoB100 was synthesized by RPE. Apolipoprotein B100, but not control mice, had cholesteryl esters and lipid particles in Bruch's membrane. Immunoreactivity of ApoB100 was present in the RPE and Bruch's membrane, but not choroidal endothelium of apoB100 mice. Ultrastructural changes were consistent with aging, but not AMD when aged up to 18 months. The induction of advanced glycation end products to alter Bruch's membrane, did not promote basal linear deposit or drusen formation.

CONCLUSIONS. Mice that produce apoB100 in the RPE and liver secrete lipoproteins into Bruch's membrane, but not to the extent that distinct features of AMD develop, which suggests that either additional lipoprotein accumulation or additional factors are necessary to initiate their formation.

Keywords: age-related macular degeneration, aging, apolipoprotein B, lipoproteins, retinal pigmented epithelium

Age-related macular degeneration is the leading cause of blindness among the elderly. While numerous genetic polymorphisms are associated with AMD risk, the precise pathophysiology remains unresolved. The Age-Related Eye Disease studies showed that antioxidant therapy slows vision loss in patients with intermediate AMD.^{1,2} Unfortunately, prevention and therapy for early disease is lacking. Treatment that is based on important pathophysiologic events will lead to effective treatment for early disease.

Drusen are a cardinal clinical sign of AMD. Histopathologically, they are extracellular accumulations within Bruch's membrane (BrM). Basal deposits are a related histopathological change that, based on their location and composition, distinguish aging from AMD. The basal laminar deposit (BlamD), which forms between the RPE cell and basement membrane, is a normal aging change early, but becomes specific for AMD when they are thick and contain cellular debris, "long spacing collagen," lipoproteins, and inflammatory proteins.³⁻¹⁶ The most sensitive and specific histopathologic marker of AMD is the basal linear deposit (BlinD), which forms in the inner collagenous layer. When advanced, BlinD are seen clinically as drusen.⁸⁻¹¹

A critical event that precedes basal deposits and drusen is the accumulation of lipoproteins within Bruch's membrane. Lipoproteins are composed principally of an apolipoprotein, triglycerides, and cholesteryl esters that are synthesized by tissues for export. The lipoproteins found within Bruch's membrane contain apolipoprotein B100,¹⁷⁻²¹ and have distinct morphology, distribution, and density profile from plasma lipoproteins.^{22,23} Due to their apoB100 backbone, they are most similar to the proatherogenic very low and low density lipoproteins, and not chylomicrons, which contain apoB48.

The accumulation of lipoproteins in Bruch's membrane is reminiscent of the "response to retention" hypothesis of atherosclerosis, which proposes that plasma lipoproteins accumulate in the arterial subendothelial space, which initiates a cascade of inflammatory events leading to plaque formation.²⁴ Despite the large number of epidemiologic studies, systemic cholesterol levels have not correlated with AMD risk, as reviewed in Curcio et al.²⁵ An alternative theory suggests that the RPE synthesizes and secretes lipoproteins into Bruch's membrane.²⁵ We, as well as the Curcio lab, have shown that RPE cells in vitro express apoB100,^{22,26-28} although in vivo evidence is lacking. In this study, we address the hypothesis that apoB100 lipoproteins accumulate in Bruch's membrane

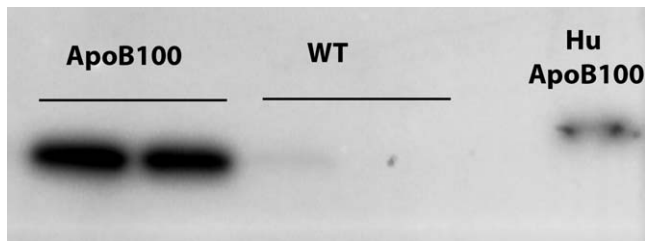


FIGURE 1. Representative Western blot of apoB100 protein from RPE-choroid extracts. A 512-kDa band from RPE-choroid extracts of apoB100 mice. A faint band and absence of a band characterize extracts from wild-type mice. The 55-kDa band from a sample of human plasma showing human apoB100 is seen in the *rightmost* lane.

and serve as a catalyst for BlinD and drusen formation. A single apoB gene encodes two isoforms, apoB100 and apoB48. In humans, apoB48 is synthesized in the small intestines and is present in chylomicrons while apoB100 is predominantly expressed by the liver. In mice, apoB48 is the major apoB form expressed in all tissues. To simulate apoB100 lipoprotein production in humans, we selected apoB100 mice that have a mutation in codon 2153 corresponding to the apoB48 editing codon, which reduces the translation of apoB48 so that apoB100 is predominantly produced.²⁹ Herein, we determined the extent the RPE *in vivo* synthesizes and secretes apoB100 lipoproteins, and whether their accumulation in Bruch's membrane induces BlinDs and drusen.

MATERIALS AND METHODS

Animals and Care

Male and female ApoB100 in a C57/S129 background or C57/S129 mice (Jackson Laboratories, Bar Harbor, ME, USA) were given standard rodent chow and water *ad libitum*, and kept in a 12-hour light-dark cycle. For studies with D-galactose, 5-month-old apoB100 mice were given daily subcutaneous injections for 8 weeks of either 0.12 mL PBS or D-galactose 50 mg/kg (Sigma-Aldrich Corp., St. Louis, MO, USA) using our published protocol.³⁰ All experiments were conducted according to the ARVO Statement for the Use of Animals in Ophthalmic and Vision Research. The research was approved by the Institutional Research Board at the Johns Hopkins University.

Tissue Preparation

After mice were killed and eyes were enucleated, one eye was fixed in 2.5% glutaraldehyde and 1% paraformaldehyde in 0.08 M cacodylate buffer for transmission electron microscopy (TEM). The central 2 × 2 mm tissue temporal to the optic nerve was postfixed with 1% osmium tetroxide, dehydrated, and embedded in Poly/Bed 812 resin (Polysciences, Inc., Warrington, PA, USA). Ultrathin sections were stained with uranyl acetate and lead citrate, and examined with an electron microscope (JEM-100 CX; JEOL, Tokyo, Japan).

Eyes were also prepared for osmium-tannic acid-paraphenylenediamine (OTAP) TEM as described, to highlight neutral lipids.^{23,31,32} Tissue was postfixed in 1% osmium in 0.1 M cacodylate buffer for 2.5 hours, 1% tannic acid (gallotannin) for 30 minutes, 1% NaSO₄ for 5 minutes, 70% ethanol (5 minutes), and 1% paraphenylenediamine in 70% ethanol for 30 minutes. Tissue was dehydrated, infiltrated, and embedded in a commercial embedding kit (PolyBed 812; Polysciences, Inc.).

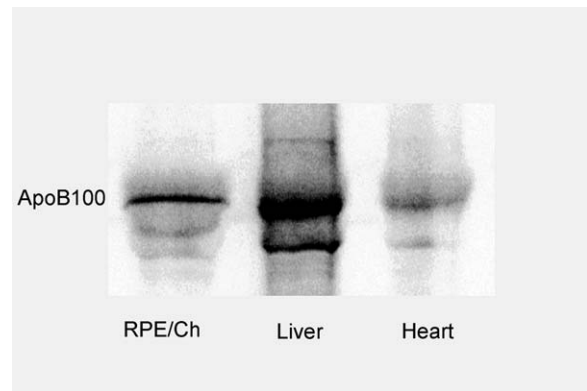


FIGURE 2. Immunoprecipitation of ³⁵S-apoB100 protein from the RPE-choroid, heart, and liver extracts of an apoB100 mouse. To confirm that the RPE-choroid synthesizes and secretes apoB100 protein, apoB100 mouse tissue extracts were prepared as described in the Methods section. A representative autoradiogram shows the immunoprecipitated radiolabeled apoB100 protein that was recovered from the supernatant. The signal from the RPE-choroid is intermediate between that of the liver and heart.

We dissected the RPE-choroid of the contralateral eye, and either used it immediately for metabolic labeling of apoB100, or it was cryopreserved at -80°C , placed in RLT lysis buffer (Qiagen, Inc., Valencia, CA, USA) or RIPA buffer with proteinase inhibitors (Sigma-Aldrich Corp.). Some eyes were fixed in 2% paraformaldehyde and cryopreserved for histochemical analysis.

Quantitative RT-PCR Analysis

We extracted total RNA from the RPE-choroid using a commercial RNA extraction kit (RNeasy Mini kit; Qiagen, Inc.) according to the manufacturer's instructions and reverse transcribed using a cDNA synthesis kit (Superscript First Strand Synthesis system; Invitrogen, Carlsbad, CA, USA). Expression was determined by RT-qPCR (LightCycler; Roche Diagnostics, Nutley, NJ, USA) as described Ishibashi et al.³³ Primers were designed with DNA sequencing software (Primer 3; Broad Institute, Cambridge, MA, USA; provided in the public domain at <http://fokker.wi.mit.edu/primer3>), and included the following primer pairs for apoB100: 5'-AAGCACCTCCGAAAGTACGTG-3'; Reverse: 5'-CTCCAGCTCTACCTTACAGTTGA-3'; MTP: Forward: 5'-ATACAAGCTCACGTACTCCACT-3'; Reverse: 5'-TCCACAGTAAACACAACGTCCA-3'; and Cyclophilin A: (Forward: 5'-CAGACGCCACTGTCGCTTTT-3'; Reverse: 5-TGTCTTTGGAACCTTGTCTGCAA-3'), which was used for normalization. Polymerase chain reaction products were quantified using the second derivative maximum values calculated with RT-PCR analysis software (LightCycler; Roche Diagnostics Corp., Indianapolis, IN, USA).

Western Blot Analysis

Western blot analysis was performed as described.³⁴ Samples (15 μg protein per lane) were separated on a 4% to 20% SDS-PAGE and electrophoretically transferred to a PVDF membrane (Bio-Rad Laboratories, Inc., Hercules, CA, USA). Membranes were incubated with a polyclonal rabbit anti-apoB antibody (1:1000; Abcam, Inc., Cambridge, MA, USA), and a secondary anti-rabbit antibody conjugated with horseradish peroxidase. Signal was detected with a chemiluminescence detection system (ECL Plus; GE-Healthcare, Piscataway, NJ, USA). Films

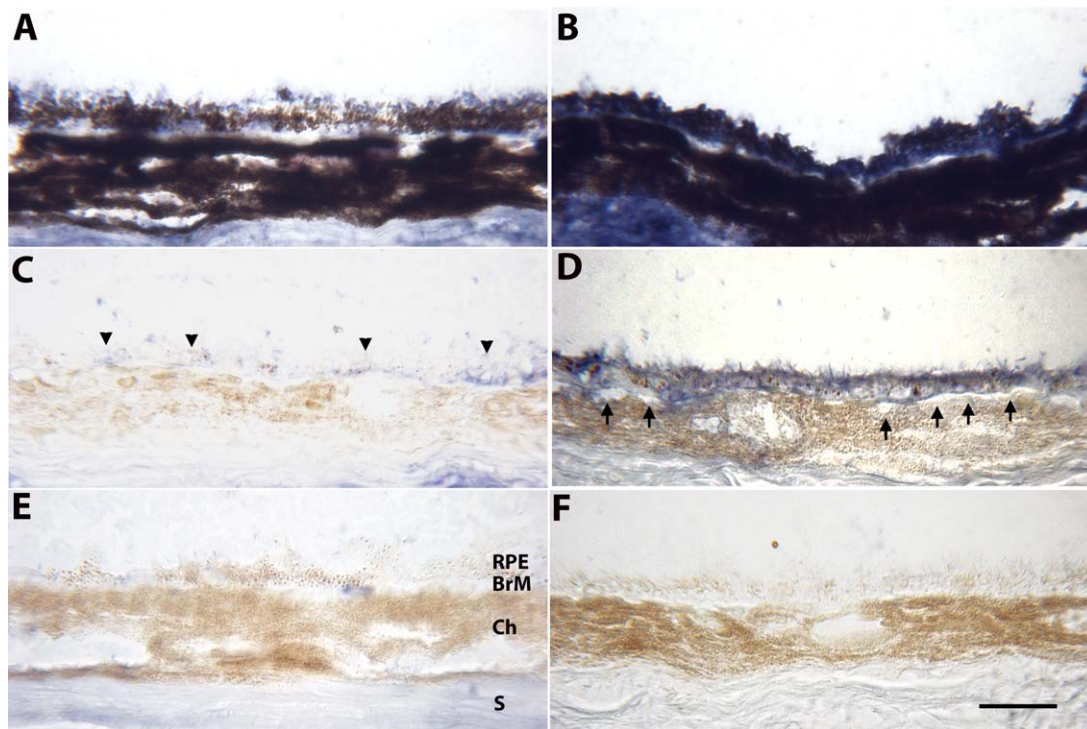


FIGURE 3. Immunohistochemistry of ApoB100 of the RPE-choroid in 2-month-old WT mice (A, C, E) and apoB100 (B, D, F) fed a normal chow diet. (A) Unbleached section from a WT mouse from a region showing some immunolabeling for apoB100, mainly in the apical regions of some RPE cells. (B) Unbleached section showing blue immunolabeling for apoB100 throughout RPE cells, which is partially obscured by melanin pigment. The sclera likely stains for apoB100, presumably from systemic deposition, as well as nonspecific staining. (C) Bleached section of a WT mouse showing mild, mosaic apoB100 immunolabeling of the RPE (arrowheads) and BrM. (D) Bleached section from an apoB100 mouse showing strong immunolabeling for apoB100 in the RPE and BrM. The staining appears in every RPE cell in the section. The choriocapillaris endothelium is quiet (arrows). (E) Bleached, nonimmune IgG control of a WT mouse showing mild background staining, especially in the sclera. (F) Bleached, nonimmune IgG control of an apoB100 mouse showing no background staining. Ch, choroid; S, sclera. Scale bar: 20 μ m.

were scanned with an image scanner (Molecular Image FX; BioRad Laboratories, Inc.).

Metabolic Labeling of ApoB100

Metabolic labeling of newly synthesized apoB100 protein secreted by the RPE-choroid was examined as described³⁵ after optimizing for small tissue quantities. The RPE-choroid from two eyes, or an equal quantity by weight of heart or liver, was minced and then washed twice with ice-cold incubation medium (methionine- and cysteine-free Dulbecco's modified Eagle's medium; Sigma-Aldrich Corp.) with 10% FBS, 1.6 mM glutamate, and 1.6 mM Na pyruvate. We added 1.0 mL of labeling medium (incubation medium containing 1.0 mCi ³⁵S-methionine/cysteine (Amersham Biosciences, Piscataway, NJ, USA), heated to 37°C, and mixed for 3 hours. The tissue was pelleted by centrifugation at 13,400 g for 1 minute, and the supernatant was collected and added to $\times 5$ NET buffer containing rabbit polyclonal anti-apoB antibody (1:1000; Abcam, Inc.) and a protease inhibitor mixture. After overnight incubation, the medium was added to protein-A agarose (Sigma-Aldrich Corp.) for 2 hours. We separated the ³⁵S-methionine-labeled immunoprecipitated apoB100 by 5% SDS-PAGE, fixed, dried, and imaged with a phosphorimager.

Cholesteryl Ester Filipin Histochemistry

To detect cholesteryl esters, cryosections (5 μ m) were warmed to room temperature, as previously described by Curcio et al.³⁶ Unesterified cholesterol was extracted with two 5-minute rinses of 70% ethanol. Cholesteryl esters were hydrolyzed with

cholesterol hydrolase (1.65 U/mL; Boehringer Mannheim, Inc., Pleasanton, CA, USA) for 3 hours at 37°C. Released cholesterol was detected by permeabilizing sections with Triton X-100 0.5% and then incubating with Filipin (60 μ g/mL; Sigma-Aldrich Corp.) for 2 hours in the dark at room temperature. Images of Filipin staining were collected on a microscope (Nikon Eclipse TE2000U; Nikon Instruments, Inc., Melville, NY, USA) using a UV-2A epifluorescence filter with EX/DM/BA of 330 to 380/400/420 nm. At least 10 sections were evaluated for each mouse.

Immunohistochemistry and Bleaching

Streptavidin alkaline phosphatase (APase) immunohistochemistry was performed on cryopreserved tissue sections using a nitroblue tetrazolium (NBT) development system, as reported previously.³⁷ In brief, 5- μ m thick cryosections were permeabilized with absolute methanol and blocked with 2% horse serum in tris-buffered saline, pH 7.4 with 1% BSA and an avidin-biotin complex (ABC) blocking kit (Vector Laboratories, Inc., Burlingame, CA, USA). Sections were incubated overnight at 4°C with a polyclonal anti-apoB100 antibody (1:50; ApoB H-15, Santa Cruz Biotechnology, Inc., Dallas, TX, USA), which is specific for mouse apoB100, or antioxidantized phospholipid E06 IgM (1:100; provided by Joe Witztum, MD, UC San Diego, San Diego, CA, USA) or normal immunoglobulin G (IgG) or IgM control, with biotinylated horse anti-goat IgG (1:4000, Vector Laboratories, Inc.) for 30 minutes, and then with ABC-APase (Vector Laboratories, Inc.). We developed APase activity with a 5-bromo-4-chloro-3-indoyl phosphate (BCIP)-NBT kit (Vector Laboratories, Inc.), yielding a blue reaction product.

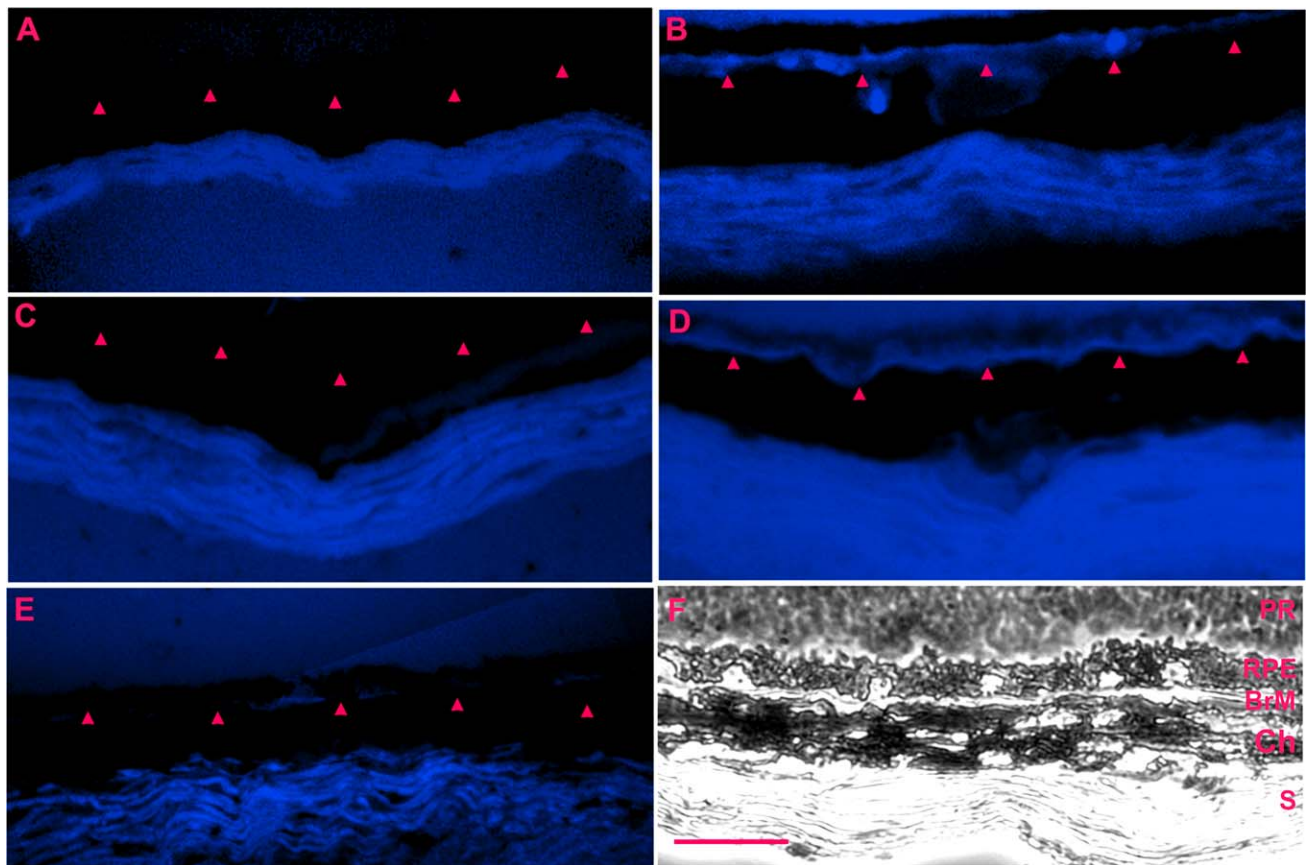


FIGURE 4. Cholesteryl esterase Filipin histochemistry of apoB100 and WT mice fed a normal chow diet. (A) 2-month-old WT mouse without blue labeling for cholesteryl esters in BrM (red arrowheads). There is nonspecific staining of the sclera. (B) A 2-month-old apoB100 mouse showing blue stripe labeling for cholesteryl esters in BrM. (C) An 8-month-old WT mouse without labeling for cholesteryl esters in BrM. (D) An 8-month-old apoB100 mouse with blue label for cholesteryl esters in BrM. (E) Section from an 8-month-old apoB100 mouse without Filipin staining shows minimal staining in BrM. (F) Brightfield image of the neurosensory retina (R), RPE, BrM, Ch, and S. Scale bar: 20 μ m.

To bleach melanin pigment in order to visualize the immunoreaction product in the RPE, sections were fixed in 4% paraformaldehyde overnight at 4°C after streptavidin APase immunohistochemistry and immersed in 0.05% potassium permanganate (Aldrich Chemical Co., Milwaukee, WI, USA) for 25 minutes, and then with 35% peracetic acid (FMC Corp., Philadelphia, PA, USA) for 15 to 20 minutes.

Statistics

At least 5 eyes from either apoB100 or control mice were used for each assay. Statistical comparisons were made between groups using the Student's unpaired *t*-test.

RESULTS

ApoB100 Mice Express ApoB100

Total RNA from the liver and RPE-choroid of 2-month-old apoB100 and wild-type (C57/129) mice ($n = 5$ each) were subjected to RT-qPCR using ApoB primers. Compared with wild-type mice, the RPE-choroid of apoB100 mice expressed 4.8-fold higher apoB ($P < 0.05$). In apoB100 mice, apoB mRNA expression of the RPE-choroid was 4.9-fold higher than the heart ($P < 0.05$), but 15.8-fold lower than the liver ($P < 0.01$). We also examined the RPE-choroid for Microsomal transfer protein (MTTP) expression since it is an enzyme required for apoB100 lipoprotein release,^{38,39} and found that MTTP

expression was 30% lower than in the liver ($n = 5$ mice; $P < 0.05$).

Conversion to apoB48 is a posttranscriptional process. Therefore, we used Western analysis to determine the extent that the RPE-choroid contained apoB100 protein. Apolipoprotein B100 was detected in the RPE-choroid of apoB100 mice ($n = 5$), but not in wild-type mice ($n = 5$; Fig. 1). Since some of the apoB100 could have originated from blood within the choriocapillaris (CC), RPE-choroids were dissected from two eyes of apoB100 and wild-type mice, and radiolabeled with ³⁵S-methionine/cysteine. The newly synthesized, radiolabeled proteins that were secreted by the RPE-choroid were immunoprecipitated with an anti-apoB100 antibody, and separated by PAGE. Autoradiograms of ³⁵S-apoB100 immunoprecipitated protein confirmed that apoB100 protein is synthesized and secreted by the RPE-choroid (Fig. 2). The experiment was repeated twice more, and the average signal intensity of ³⁵S-apoB100/total cell protein secreted into the medium by the RPE-choroid from the three experiments was 4.3-fold less than the liver ($P < 0.05$), but 2-fold greater than that secreted by the heart ($P < 0.05$).

To topographically localize apoB100, immunohistochemistry was performed using an antibody that recognizes the carboxy-terminal portion of the mouse apoB protein so that apoB100 but not apoB48 is labeled. Two-month-old apoB100 mice ($n = 5$) showed consistent immunolabeling in the RPE and Bruch's membrane (Fig. 3). The choriocapillaris endothelium did not immunostain for apoB100. Similarly aged WT mice



($n = 5$) showed a mosaic pattern of immunolabeling for apoB100 in the RPE and Bruch's membrane. Similar staining patterns were seen in 8-month-old apoB100 ($n = 5$) and WT mice ($n = 5$; data not shown).

Bruch's Membrane Accumulates Neutral Lipids

Filipin histochemistry is specific for cholesterol. Prior tissue treatment with cholesteryl esterase assesses cholesteryl esters, which in the extracellular space, are contained only in lipoproteins.³⁶ Figure 4 shows staining for cholesteryl esters in Bruch's membrane of 2-month-old apoB100 mice ($n = 5$) while 2-month-old wild-type mice ($n = 5$) showed no staining. Older 8-month-old apoB100 mice ($n = 5$) also had a prominent line of filipin staining in Bruch's membrane (Fig. 4). No staining was seen in 8-month-old WT mice ($n = 5$).

A lipid preserving technique, OTAP TEM, was used to visualize lipid inclusions within Bruch's membrane of 2-month-old ($n = 5$) apoB100 mice. Figure 5 shows electron dense particles, 60 to 310 nm in diameter, within Bruch's membrane of apoB100 mice. Electron dense particles were not found in Bruch's membrane of WT mice. Collectively, these data suggest that apoB100 lipoproteins accumulate in Bruch's membrane of apoB100 mice.

Lack of an AMD Phenotype With Aging

With evidence of lipoprotein synthesis by the RPE and lipoprotein accumulation in Bruch's membrane, we next aged the animals to determine the extent that BlinDs and drusen develop. We also looked for RPE changes such as basolateral infoldings loss, a marker of epithelial injury,⁴⁰⁻⁴² and cytoplasmic vacuoles, which develop in the RPE that overlie drusen,⁵ as indicators of RPE degeneration associated with AMD. The retinal pigment epithelium of 12-month-old WT ($n = 5$) and apoB100 mice ($n = 5$) fed a normal chow diet appeared healthy (Fig. 6). Bruch's membrane maintained a pentalaminar structure composed of the RPE basement membrane, inner collagenous layer, middle elastic layer, outer collagenous layer, and choriocapillaris basement membrane. When present, basal laminar deposits were thin and of homogeneous composition, which is characteristic of aging, but not AMD. Outer collagenous layer deposits and reduplication of the choriocapillaris basement membrane, both normal aging changes,^{43,44} were also present. The choriocapillaris endothelium appeared healthy with fenestrations. Neither the 12-month-old WT nor apoB100 mice showed immunohistochemical evidence of oxidized LDL in Bruch's membrane using the E06 antibody or complement C3 as an indicator of complement activation (not shown). Likewise, RPE apoptosis, a hallmark change in AMD,⁴ was not observed with TUNEL labeling (data not shown).

We therefore, aged mice until 18 months, and found that the RPE of WT ($n = 5$) and apoB100 mice ($n = 5$) had normal appearing RPE with preserved basolateral infoldings, and minimal to no cytoplasmic membranous vacuoles (Fig. 7). Bruch's membrane had thin, homogeneous basal laminar deposits, and did not display labeling for oxidized lipoproteins

FIGURE 5. Transverse electron microscopy with OTAP labeling solid lipid-filled particles. (A) A 2-month-old WT mouse fed a normal diet shows no solid particles. (B) A 2-month-old apoB100 mouse. Arrows point to two small solid particles that measure 95 nm and the larger particle is 125 nm in diameter (black arrows). (C) A different 2-month-old apoB100 mouse on a normal diet shows multiple solid particles (some indicated by white arrows) that measure from 60 to 200 nm. Scale bar: 500 nm.

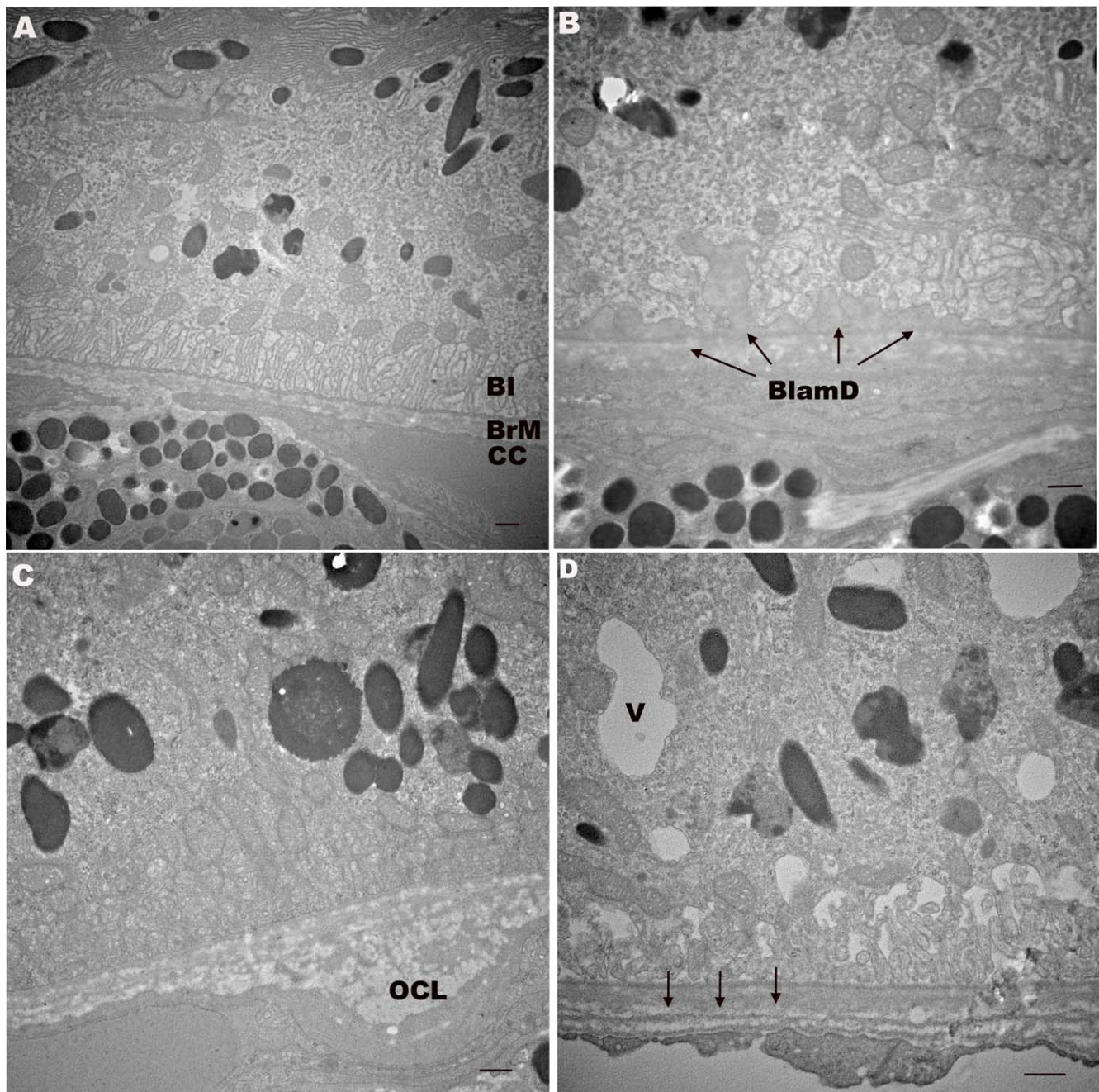


FIGURE 6. Transverse electron microscopy of 12-month-old apoB100 mice show aging, but not AMD changes. (A) A 12-month-old WT mouse with normal RPE including basal infoldings (BI), BrM, and CC endothelium. (B) A 12-month-old apoB100 mouse with preserved RPE including mitochondria and BI. Thin, homogeneous BlamDs appear between the RPE and its basement membrane (arrows). (C) A 12-month-old apoB100 mouse with outer collagenous layer (OCL) deposit, a normal aging change. (D) A 12-month-old apoB100 mouse with small cytoplasmic vacuole (V). Bruch's membrane has a redundant choriocapillaris basement membrane (arrows). Scale bar: 300 nm.

or basal deposits, C3 immunolabeling, or evidence of RPE apoptosis (data not shown).

Lack of BlinD or Drusen Formation With AGE Formation

We previously showed that D-galactose treatment in mice induces advanced glycation endproduct (AGE) formation in Bruch's membrane and elements of AMD including basal laminar deposits with heterogeneous debris, but not BlinDs or

drusen.³⁰ We also showed that AGE formation in this model induces lipoprotein lipase production, which contributes to lipoprotein retention.⁴⁵ We hypothesized that Bruch's membrane modifications from AGE formation would increase lipoprotein retention, leading to BlinDs and drusen. As seen in Figure 8, one month following D-galactose treatment,³⁰ we found that D-galactose treated apoB100 mice had a similar degree of solid lipid particles in Bruch's membrane as PBS-treated mice. Apolipoprotein B100-mice treated with D-galactose developed thin basal laminar deposits and outer

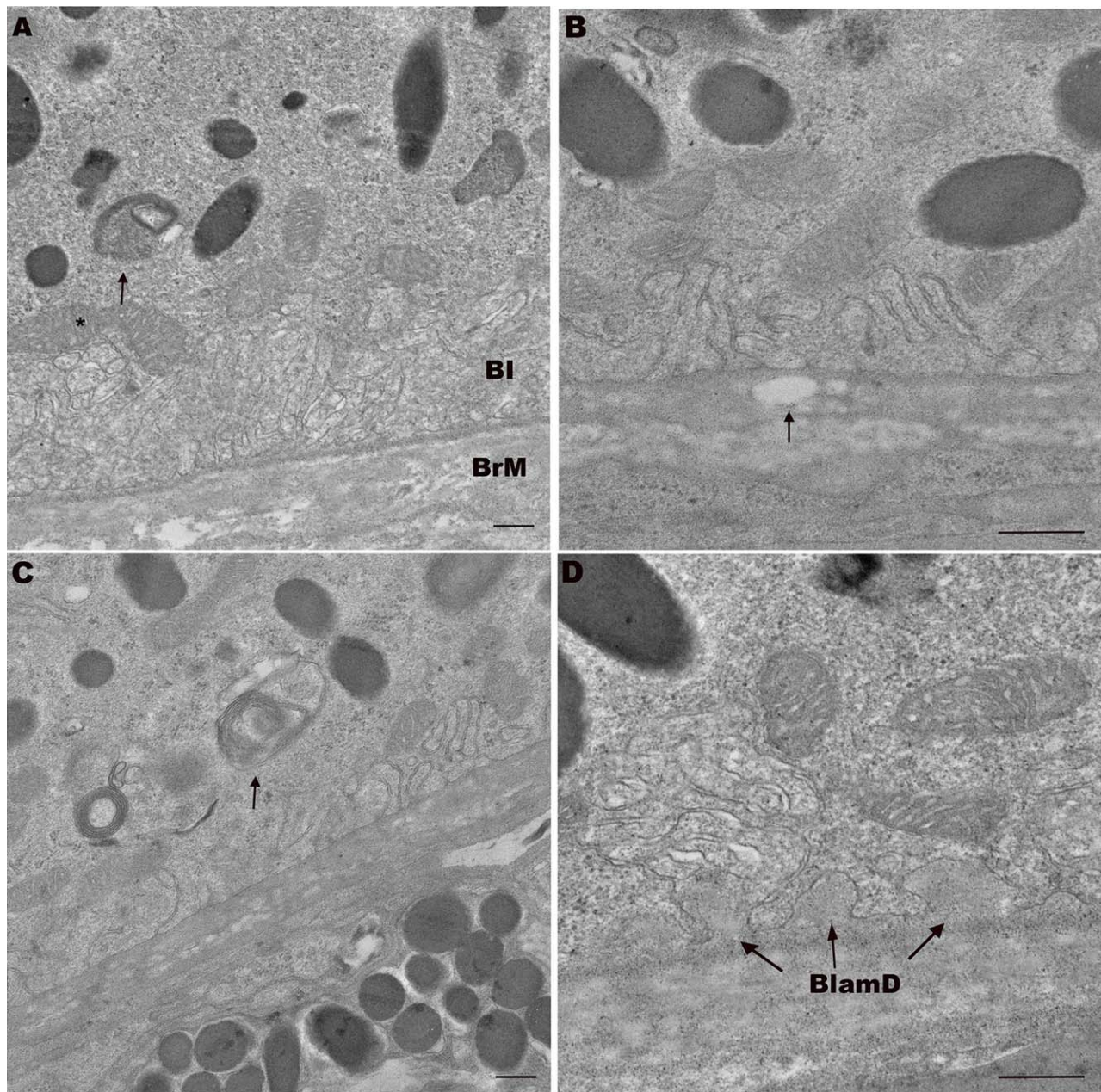


FIGURE 7. Transverse electron microscopy of 18-month-old ApoB100 mice shows aging, but no AMD changes. (A) An 18-month-old WT mouse with normal appearing RPE including mitochondria (*) and Bl, and BrM. Note undigested photoreceptor outer segment (arrow). (B) An 18-month-old apoB100 mouse with preserved RPE Bl. Bruch's membrane has a vacuole that is suggestive of lipid accumulation (arrow). (C) An 18-month-old apoB100 mouse with mild RPE abnormality including partially digested photoreceptor outer segment (arrow) in the basal RPE. Note the preserved basal infoldings. (D) An 18-month-old apoB100 mouse with preserved RPE and thin, homogeneous basal laminar deposits (BlamD, arrows). Scale bar: 300 nm.

collagenous layer deposits, which are signs of aging, but not BlinDs or drusen (Fig. 9).

DISCUSSION

Herein, we demonstrate that the RPE-choroid of apoB100 mice produce measurable apoB100. Our transcriptional and metabolic labeling studies show that the RPE-choroid synthesizes and secretes apoB100 protein while our immunohistochemical evaluation identified apoB100 in the RPE and not the choriocapillaris endothelium, which indicates that the RPE produces apoB100. This scenario provides in vivo

support for the observations of apoB100 production by RPE cells in vitro,^{22,28,46} and supports the theory that lipoproteins accumulated in Bruch's membrane could originate from the RPE and/or liver.^{22,26,46} This scenario is in contrast to most mice, which predominantly produce apoB48, and less apoB100. Since apoB100 and not apoB48 containing lipoproteins have been identified in human Bruch's membrane, drusen, and basal deposits in aging and AMD, we believe this model is suitable to study the extent that apoB100 lipoprotein particles are mechanistically involved in the pathogenesis of AMD.

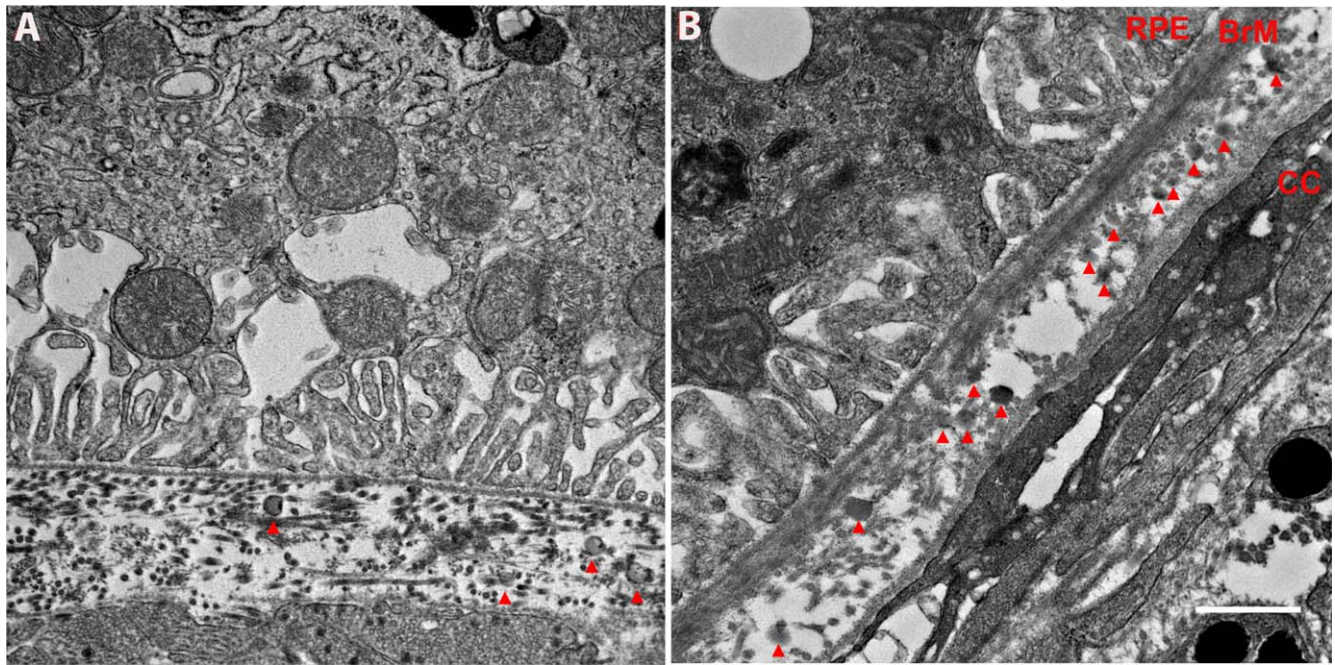


FIGURE 8. Transverse electron microscopy with OTAP labeling solid lipid-filled particles after apoB100 mice were treated with D-galactose. (A) An 8-month-old apoB100 mouse treated with PBS has solid particles (red arrowheads) that measure 95 to 125 μm in diameter in Bruch's membrane. (B) An 8-month-old apoB100 mouse treated with D-galactose has solid lipoprotein particles (red arrowheads) as well. Scale bar: 500 nm.

The “response-to-retention” hypothesis of atherosclerosis proposes that plasma lipoproteins cross the arterial vascular endothelium into the subendothelial matrix. This process is not pathologic unless the lipoproteins are retained and oxidized to generate tissue-damaging inflammation. An intracellular “response-to-retention” hypothesis would be triggered with an age-related lipoprotein accumulation in Bruch's membrane that originate from the RPE²⁵ and/or the systemic

circulation. We found the accumulation of cholesteryl esters by cholesterol ester/Filipin assay, solid lipid vesicles using OTAP TEM, and apoB100 by immunohistochemistry in Bruch's membrane of apoB100 mice from as early as age 2 months. Since neutral lipids in the extracellular matrix are contained in lipoproteins,³⁶ collectively, these results suggest that apoB100 lipoproteins accumulate from an early age. Despite this early accumulation, we did not identify BlinDs or drusen in apoB100

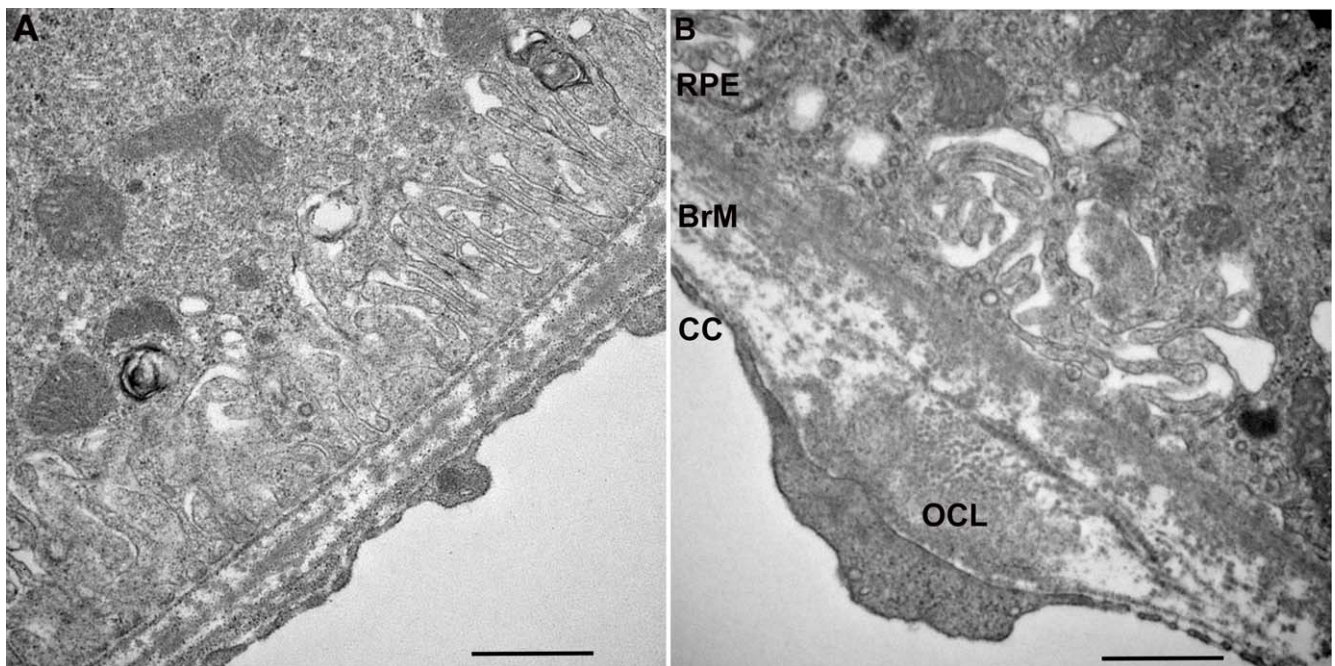


FIGURE 9. Transverse electron microscopy of ApoB100 mice treated with D-galactose show aging, but no AMD changes. (A) An 8-month-old ApoB100 mouse treated with PBS has normal RPE with preserved basolateral infoldings, and Bruch's membrane. (B) An 8-month-old apoB100 mouse treated with D-galactose shows mild derangement of RPE basolateral infoldings and an OCL deposit in Bruch's membrane. Scale bar: 500 nm.

mice aged up to 18 months. Thus, using this model, our hypothesis is disproved, as lipoprotein deposition is not sufficient for developing Bruch's membrane changes associated with AMD.

We offer several explanations for the lack of AMD phenotype. First, while lipoproteins accumulated in Bruch's membrane from an early age, they did not accumulate with aging or develop into a "lipid wall," as described in humans by Ruberti et al.,²⁰ thus falling below a threshold needed for BlinD or drusen formation. It is possible that feeding mice a high-fat diet would stimulate lipoprotein production, and thereby increase lipoprotein accumulation. We previously showed that mice, which express human apoB100, given a high-fat diet for 12 months, developed BlinDs, but no drusen.⁴⁷ In these mice, the expression of human apoB100 is driven by a liver-specific promoter that promotes hyperlipidemia, but likely with minimal production by the RPE.⁴⁸ It is possible that the total lipoprotein accumulation fell below the threshold that drives drusenogenesis due to the lack of lipoprotein production by the RPE.

Second, an obvious shortcoming of using mice to study AMD is that mice lack maculas. Human maculas are enriched in cone photoreceptors—and cone outer segments, relative to rods, contain more unesterified cholesterol.⁴⁹ In humans, BlinDs develop in the fovea, coinciding with cone-rich photoreceptors though they do not develop in the periphery where cholesterol poor rods predominate.^{50,51} The macular RPE cell, after phagocytosing cone outer segments, is burdened with an additional cholesterol load from a high-fat diet and will package unwanted cholesterol into lipoproteins for basolateral release into the choriocapillaris. This response would be analogous to cardiac myocytes that secrete lipoproteins to remove excess cellular cholesterol and prevent lipoprotein retention, which can prevent cardiac failure.⁵²⁻⁵⁴ Because the mouse neurosensory retina is rod-rich,⁵⁵ which simulates the human peripheral retina, the cholesterol burden of the RPE is derived only from the diet and not from outer segment phagocytosis, resulting in lipoprotein production that will fall below the threshold necessary for oxidation to generate inflammation. In support of this theory, we did not find any evidence of lipoprotein oxidation using E06 immunolabeling or complement activation using C3 as a marker.

Third, it is conceivable that aging changes to Bruch's membrane were inadequate to induce lipoprotein retention. We previously showed that altering Bruch's membrane with AGEs, which accumulate with aging and AMD,⁵⁶ causes the acute retention of intravenously injected lipoproteins in Bruch's membrane.⁴⁵ Treating apoB100 mice with D-galactose resulted in aging associated BlinD and outer collagenous layer deposits, but not BlinDs or drusen. These changes in 8-month-old mice were similar to 18-month-old apoB100 mice. While treatment with D-galactose accelerated aging, the ultrastructural changes were comparable with those in WT mice treated with D-galactose.³⁰ We suggest that D-galactose induced Bruch's membrane changes that were sufficient to promote acute lipoprotein retention, but inadequate chronically to induce sufficient accumulation that added to the phenotype induced by D-galactose treatment in the absence of lipoproteins. In this regard, we recognize that aging mice beyond 18 months might promote sufficient Bruch's membrane aging to drive drusenogenesis.

Finally, it is possible that the degree of oxidative stress was insufficient to oxidize Bruch's membrane lipoproteins. Previously, we showed basal deposit formation in C57Bl6J mice exposed to cigarette smoke, the strongest environmental risk factor for AMD risk, and a strong chemical oxidant,⁵⁷⁻⁵⁹ suggesting that smoking-related oxidative stress induces Bruch's membrane changes. While we did not attempt to

determine the source of Bruch's membrane lipoproteins, lipoprotein production by both the eye and liver mirrors their origin in humans. Thus, this model will be valuable for testing whether any of the above possibilities are involved in BlinD and drusen formation.

Acknowledgments

Supported by Grant EY14005 (JTH); Research to Prevent Blindness Senior Scientist Award (JTH); an unrestricted grant from Research to Prevent Blindness; and gifts from the Merlau Family and Aleda Wright. Dr. Handa is the Robert Bond Welch Professor. The authors alone are responsible for the content and writing of the paper.

Disclosure: **M. Fujihara**, None; **M. Cano**, None; **J.T. Handa**, None

References

1. Age-Related Eye Disease Study Research Group. A randomized, placebo-controlled, clinical trial of high-dose supplementation with vitamins C and E, beta carotene, and zinc for age-related macular degeneration and vision loss: AREDS report no. 8. *Arch Ophthalmol*. 2001;119:1417-1436.
2. Lutein + zeaxanthin and omega-3 fatty acids for age-related macular degeneration: the Age-Related Eye Disease Study 2 (AREDS2) randomized clinical trial. *JAMA*. 2013;309:2005-2015.
3. Del Priore LV, Kuo YH, Tezel TH. Age-related changes in human RPE cell density and apoptosis proportion in situ. *Invest Ophthalmol Vis Sci*. 2002;43:3312-3318.
4. Dunaief JL, Dentichev T, Ying GS, Milam AH. The role of apoptosis in age-related macular degeneration. *Arch Ophthalmol*. 2002;120:1435-1442.
5. Anderson DH, Mullins RF, Hageman GS, Johnson LV. A role for local inflammation in the formation of drusen in the aging eye. *Am J Ophthalmol*. 2002;134:411-431.
6. Sarks SH. Ageing and degeneration in the macular region: a clinico-pathological study. *Br J Ophthalmol*. 1976;60:324-341.
7. Johnson LV, Leitner WP, Rivest AJ, Staples MK, Radeke MJ, Anderson DH. The Alzheimer's A beta -peptide is deposited at sites of complement activation in pathologic deposits associated with aging and age-related macular degeneration. *Proc Natl Acad Sci U S A*. 2002;99:11830-11835.
8. Curcio CA, Millican CL. Basal linear deposit and large drusen are specific for early age-related maculopathy. *Arch Ophthalmol*. 1999;117:329-339.
9. Green WR, Enger C. Age-related macular degeneration histopathologic studies. The 1992 Lorenz E. Zimmerman lecture. *Ophthalmology*. 1993;100:1519-1535.
10. Spraul CW, Grossniklaus HE. Characteristics of Drusen and Bruch's membrane in postmortem eyes with age-related macular degeneration. *Arch Ophthalmol*. 1997;115:267-273.
11. Spraul CW, Lang GE, Grossniklaus HE. Morphometric analysis of the choroid, Bruch's membrane, and retinal pigment epithelium in eyes with age-related macular degeneration. *Invest Ophthalmol Vis Sci*. 1996;37:2724-2735.
12. Leu ST, Batni S, Radeke MJ, Johnson LV, Anderson DH, Clegg DO. Drusen are cold spots for proteolysis: expression of matrix metalloproteinases and their tissue inhibitor proteins in age-related macular degeneration. *Exp Eye Res*. 2002;74:141-154.
13. Newsome DA, Hewitt AT, Huh W, Robey PG, Hassell JR. Detection of specific extracellular matrix molecules in drusen, Bruch's membrane, and ciliary body. *Am J Ophthalmol*. 1987;104:373-381.
14. van der Schaft TL, Mooy CM, de Bruijn WC, Bosman FT, de Jong PT. Immunohistochemical light and electron microscopy of basal laminar deposit. *Graefes Arch Clin Exp Ophthalmol*. 1994;32:40-46.

15. Feeney-Burns L, Burns RP, Gao CL. Age-related macular changes in humans over 90 years old. *Am J Ophthalmol*. 1990;109:265-278.
16. Loffler KU, Lee WR. Basal linear deposit in the human macula. *Graefes Arch Clin Exp Ophthalmol*. 1986;24:493-501.
17. Curcio CA, Millican CL, Bailey T, Kruth HS. Accumulation of cholesterol with age in human Bruch's membrane. *Invest Ophthalmol Vis Sci*. 2001;42:265-274.
18. Holz FG, Sheraidah G, Pauleikhoff D, Bird AC. Analysis of lipid deposits extracted from human macular and peripheral Bruch's membrane. *Arch Ophthalmol*. 1994;112:402-406.
19. Pauleikhoff D, Harper CA, Marshall J, Bird AC. Aging changes in Bruch's membrane. A histochemical and morphologic study. *Ophthalmology*. 1990;97:171-178.
20. Ruberti JW, Curcio CA, Millican CL, Menco BP, Huang JD, Johnson M. Quick-freeze/deep-etch visualization of age-related lipid accumulation in Bruch's membrane. *Invest Ophthalmol Vis Sci*. 2003;44:1753-1759.
21. Haimovici R, Gantz DL, Rumelt S, Freddo TF, Small DM. The lipid composition of drusen, Bruch's membrane, and sclera by hot stage polarizing light microscopy. *Invest Ophthalmol Vis Sci*. 2001;42:1592-1599.
22. Li CM, Presley JB, Zhang X, et al. Retina expresses microsomal triglyceride transfer protein: implications for age-related maculopathy. *J Lipid Res*. 2005;46:628-640.
23. Curcio CA, Presley JB, Millican CL, Medeiros NE. Basal deposits and drusen in eyes with age-related maculopathy: evidence for solid lipid particles. *Exp Eye Res*. 2005;80:761-775.
24. Williams KJ, Tabas I. The response-to-retention hypothesis of early atherogenesis. *Arterioscler Thromb Vasc Biol*. 1995;15:551-561.
25. Curcio CA, Johnson M, Huang JD, Rudolf M. Aging, age-related macular degeneration, and the response-to-retention of apolipoprotein B-containing lipoproteins. *Prog Retin Eye Res*. 2009;28:393-422.
26. Malek G, Li CM, Guidry C, Medeiros NE, Curcio CA. Apolipoprotein B in cholesterol-containing drusen and basal deposits of human eyes with age-related maculopathy. *Am J Pathol*. 2003;162:413-425.
27. Ishida BY, Bailey KR, Duncan KG, et al. Regulated expression of apolipoprotein E by human retinal pigment epithelial cells. *J Lipid Res*. 2004;45:263-271.
28. Wu T, Tian J, Cutler RG, et al. Knockdown of FABP5 mRNA decreases cellular cholesterol levels and results in decreased apoB100 secretion and triglyceride accumulation in ARPE-19 cells. *Lab Invest*. 2010;90:963-965.
29. Farese RV Jr, Veniant MM, Cham CM, et al. Phenotypic analysis of mice expressing exclusively apolipoprotein B48 or apolipoprotein B100. *Proc Natl Acad Sci U S A*. 1996;93:6393-6398.
30. Ida H, Ishibashi K, Reiser K, Hjelmeland LM, Handa JT. Ultrastructural Aging of the RPE-Bruch's membrane-choriocapillaris complex in the d-galactose-treated mouse. *Invest Ophthalmol Vis Sci*. 2004;45:2348-2354.
31. Guyton JR, Klemp KF. Ultrastructural discrimination of lipid droplets and vesicles in atherosclerosis: value of osmium-thiocarbohydrazide-osmium and tannic acid-paraphenylenediamine techniques. *J Histochem Cytochem*. 1988;36:1319-1328.
32. Dithmar S, Curcio CA, Le NA, Brown S, Grossniklaus HE. Ultrastructural changes in Bruch's membrane of apolipoprotein E-deficient mice. *Invest Ophthalmol Vis Sci*. 2000;41:2035-2042.
33. Ishibashi K, Tian J, Handa JT. Similarity of mRNA phenotypes of morphologically normal macular and peripheral retinal pigment epithelial cells in older human eyes. *Invest Ophthalmol Vis Sci*. 2004;45:3291-3301.
34. Handa JT, Reiser KM, Matsunaga H, Hjelmeland LM. The advanced glycation endproduct pentosidine induces the expression of PDGF-B in human retinal pigment epithelial cells. *Exp Eye Res*. 1998;66:411-419.
35. Boren J, Veniant MM, Young SG. Apo B100-containing lipoproteins are secreted by the heart. *J Clin Invest*. 1998;101:1197-1202.
36. Curcio CA, Presley JB, Malek G, Medeiros NE, Avery DV, Kruth HS. Esterified and unesterified cholesterol in drusen and basal deposits of eyes with age-related maculopathy. *Exp Eye Res*. 2005;81:731-741.
37. Bhutto IA, Kim SY, McLeod DS, et al. Localization of collagen XVIII and the endostatin portion of collagen XVIII in aged human control eyes and eyes with age-related macular degeneration. *Invest Ophthalmol Vis Sci*. 2004;45:1544-1552.
38. Wetterau JR, Aggerbeck LP, Bouma ME, et al. Absence of microsomal triglyceride transfer protein in individuals with abetalipoproteinemia. *Science*. 1992;258:999-1001.
39. Gordon DA, Jamil H, Sharp D, et al. Secretion of apolipoprotein B-containing lipoproteins from HeLa cells is dependent on expression of the microsomal triglyceride transfer protein and is regulated by lipid availability. *Proc Natl Acad Sci U S A*. 1994;91:7628-7632.
40. Olsen TS, Wassef NF, Olsen HS, Hansen HE. Ultrastructure of the kidney in acute interstitial nephritis. *Ultrastruct Pathol*. 1986;10:1-16.
41. Olsen S, Burdick JF, Keown PA, Wallace AC, Racusen LC, Solez K. Primary acute renal failure ("acute tubular necrosis") in the transplanted kidney: morphology and pathogenesis. *Medicine (Baltimore)*. 1989;68:173-187.
42. Druce T, Hennessen U, Nabarra B, et al. Ultrastructural and functional abnormalities of intestinal and renal epithelium in the SHR. *Kidney Int*. 1990;37:1438-1448.
43. Killingsworth MC. Age-related components of Bruch's membrane in the human eye. *Graefes Arch Clin Exp Ophthalmol*. 1987;25:406-412.
44. Marshall GE, Konstas AG, Reid GG, Edwards JG, Lee WR. Collagens in the aged human macula. *Graefes Arch Clin Exp Ophthalmol*. 1994;32:133-140.
45. Cano M, Fijalkowski N, Kondo N, Dike S, Handa J. Advanced glycation endproduct changes to Bruch's membrane promotes lipoprotein retention by lipoprotein lipase. *Am J Pathol*. 2011;179:850-859.
46. Li CM, Clark ME, Chimento MF, Curcio CA. Apolipoprotein localization in isolated drusen and retinal apolipoprotein gene expression. *Invest Ophthalmol Vis Sci*. 2006;47:3119-3128.
47. Fujihara M, Bartels E, Nielsen LB, Handa JT. A human apoB100 transgenic mouse expresses human apoB100 in the RPE and develops features of early AMD. *Exp Eye Res*. 2009;88:1115-1123.
48. Callow MJ, Stoltzfus LJ, Lawn RM, Rubin EM. Expression of human apolipoprotein B and assembly of lipoprotein(a) in transgenic mice. *Proc Natl Acad Sci U S A*. 1994;91:2130-2134.
49. Albert AD, Boesze-Battaglia K. The role of cholesterol in rod outer segment membranes. *Prog Lipid Res*. 2005;44:99-124.
50. Curcio CA, Sloan KR, Kalina RE, Hendrickson AE. Human photoreceptor topography. *J Comp Neurol*. 1990;292:497-523.
51. Curcio CA, Messinger JD, Sloan KR, McGwin G, Medeiros NE, Spaide RF. Subretinal drusenoid deposits in non-neovascular age-related macular degeneration: morphology, prevalence, topography, and biogenesis model. *Retina*. 2013;33:265-276.
52. Nielsen LB, Veniant M, Boren J, et al. Genes for apolipoprotein B and microsomal triglyceride transfer protein are expressed in the heart: evidence that the heart has the capacity to synthesize and secrete lipoproteins. *Circulation*. 1998;98:13-16.

53. Nielsen LB, Bartels ED, Bollano E. Overexpression of apolipoprotein B in the heart impedes cardiac triglyceride accumulation and development of cardiac dysfunction in diabetic mice. *J Biol Chem*. 2002;277:27014-27020.
54. Yokoyama M, Yagyu H, Hu Y, et al. Apolipoprotein B production reduces lipotoxic cardiomyopathy: studies in heart-specific lipoprotein lipase transgenic mouse. *J Biol Chem*. 2004;279:4204-4211.
55. Carter-Dawson LD, LaVail MM. Rods and cones in the mouse retina. I. Structural analysis using light and electron microscopy. *J Comp Neurol*. 1979;188:245-262.
56. Farboud B, Aotaki-Keen A, Miyata T, Hjelmeland LM, Handa JT. Development of a polyclonal antibody with broad epitope specificity for advanced glycation endproducts and localization of these epitopes in Bruch's membrane of the aging eye. *Mol Vis*. 1999;5:11.
57. Tomany SC, Wang JJ, Van Leeuwen R, et al. Risk factors for incident age-related macular degeneration: pooled findings from 3 continents. *Opthalmology*. 2004;111:1280-1287.
58. Church DF, Pryor WA. Free-radical chemistry of cigarette smoke and its toxicological implications. *Environ Health Perspect*. 1985;64:111-126.
59. Fujihara M, Nagai N, Sussan TE, Biswal S, Handa JT. Chronic cigarette smoke causes oxidative damage and apoptosis to retinal pigmented epithelial cells in mice. *PLoS One*. 2008;3:e3119.